Leading Baryon Production at HERA

William B. Schmidke[1] *and Armen Bunyatyan*[2] *(on behalf of the H1 and ZEUS collaborations)*
[1]MPI, Munich, [2]MPI, Heidelberg and Yerevan Physics Institute, Yerevan, Armenia

Abstract
Data from leading baryon production at HERA are presented and compared to models. Standard string fragmentation models alone do not describe the data; models including also baryon production via virtual meson exchange give a good description of the data. Exchange models accounting for absorption describe the Q^2 evolution of the data. In the exchange picture, leading neutron data are used to extract the pion structure function.

1 Introduction

Events with a baryon carrying a large fraction of the proton beam energy have been observed in ep scattering at HERA [1]. The dynamical mechanisms for their production are not completely understood. They may be the result of hadronization of the proton remnant, conserving baryon number in the final state. Exchange of virtual particles is also expected to contribute. In this picture, the target proton fluctuates into a virtual meson-baryon state. The virtual meson scatters with the projectile lepton, leaving the fast forward baryon in the final state. Leading neutron (LN) production occurs through the exchange of isovector particles, notably the π^+ meson. For leading proton (LP) production isoscalar exchange also contributes, including diffraction mediated by Pomeron exchange. In the exchange picture, the cross section for some process in ep scattering with e.g. LN production factorizes:

$$\sigma_{ep\to enX} = f_{\pi/p}(x_L, t) \cdot \sigma_{e\pi\to eX}.$$

Here $f_{\pi/p}$ is the flux of virtual pions in the proton, $x_L = E_n/E_p$ is the fraction of the proton beam energy carried by the neutron, and t is the virtuality of the exchanged pion.

The H1 and ZEUS experiments at HERA measured leading baryons in deep inelastic scattering and photoproduction events. Leading protons were measured with position sensitive detectors placed along the proton beam downstream of the interaction point. Leading neutrons were measured with lead-scintillator calorimeters at the zero-degree point after the proton beam was bent vertically; magnet apertures limited neutron detection to scattering angles less than 0.75 mrad.

2 Leading neutron production and models

Figure 1 shows the LN x_L distribution (left) and p_T^2 distributions in bins of x_L (right). The x_L distribution rises from lowest x_L because of the increasing p_T^2 range due to the angle limit, and then falls to zero at the kinematic limit $x_L = 1$. The p_T^2 distributions are well described by exponentials; thus the parameterization $d^2\sigma/dx_L dp_T^2 \propto a(x_L)\exp(-b(x_L)p_T^2)$ fully characterizes the two dimensional distribution.

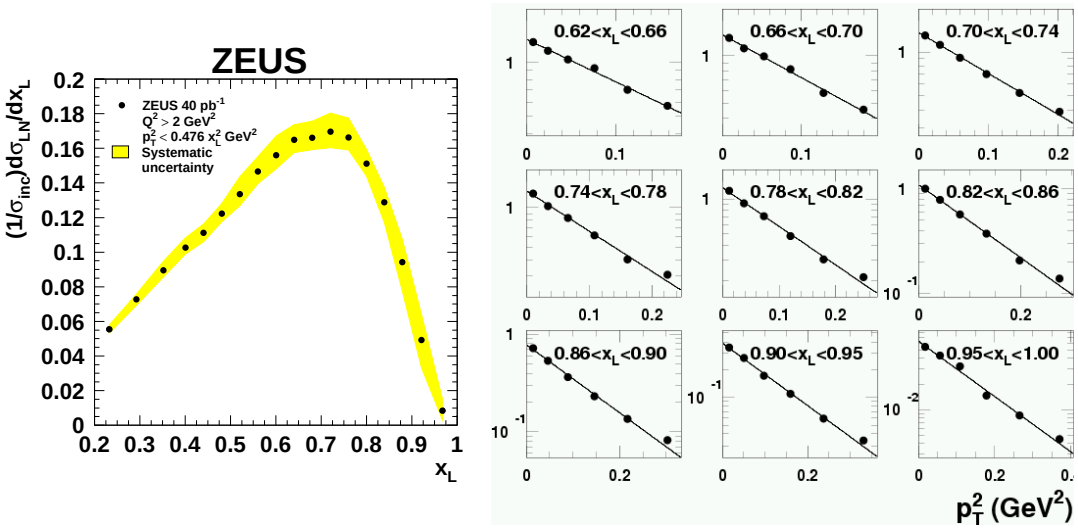

Fig. 1: Left: LN x_L distribution. Right: LN p_T^2 distributions in bins of x_L. The lines are the result of exponential fits.

The left side of Fig. 2 shows the LN x_L, intercept a and slope b distributions compared to several models. The standard fragmentation models implemented in RAPGAP and LEPTO do not describe the data, predicting too few neutrons, concentrated at lower x_L, and slopes too small and independent of x_L. The LEPTO model with soft color interactions gives a fair description of the x_L distribution and overall rate, but also fails to describe the slopes. The RAPGAP model mixing standard fragmentation and pion exchange gives a better description of the shape of the x_L distribution, and also predicts the rise of the slopes with x_L, although both with too high values. The right side of Fig. 2 shows the x_L distribution with an optimized mixture of standard fragmentation and pion exchange; the agreement with the data is very good.

3 Leading proton production and models

Figure 3 shows the x_L distribution for leading protons and neutrons in the same p_T range. If LP production proceeded only through isovector exchange, as LN production must, there should be half as many LP and LN. The data instead has approximately twice as many LP as LN. Thus, exchanges of particles with different isospins such as isoscalars must be invoked for LP production.

The left side of Fig. 4 shows a comparison of the LP x_L distributions and p_T^2 exponential slopes b to the DJANGOH and RAPGAP Monte Carlo models incorporating standard fragmentation or soft color interactions, none of which describe the data. The right side of Fig. 4 shows a comparison to a model including exchange of both isovector and isoscalar particles, including the Pomeron for diffraction [2]. These exchanges combine to give a good description of the the x_L distribution and slopes.

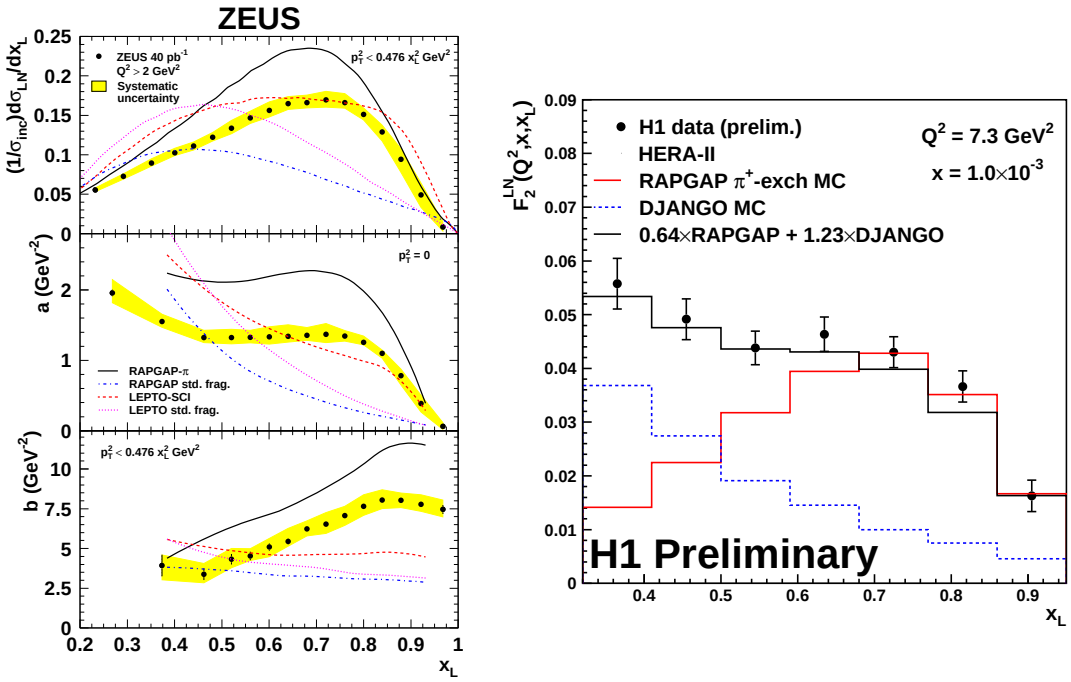

Fig. 2: Left: LN x_L, intercept and slope distributions compared to models. Right: LN x_L distribution with an optimized mixture of exchange and fragmentation models.

4 Absorption of leading neutrons

The evidence for particle exchange in leading baryon production motivates further investigation of the model. One refinement of the simple picture described in the introduction is absorption, or rescattering [3]. In this process, the virtual baryon also scatters with the projectile lepton. The baryon may migrate to lower x_L or higher p_T such that it is outside of the detector acceptance, resulting in a relative depletion of observed forward baryons. The probability of this should increase with the size of the exchanged photon. The size of the photon is inversely related to its virtuality Q^2, so the amount of absorption should increase with decreasing Q^2.

The left side of Fig. 5 shows the LN x_L spectra for photoproduction ($Q^2 \sim 0$) and three bins of increasing Q^2. The yield of LN increases monotonically with Q^2, in agreement with the expectation of the decrease of loss through absorption as Q^2 rises. The right side of Fig. 5 shows photoproduction data with two predictions from models of exchange with absorption [4]. The dashed curve model incorporates pion exchange with absorption, accounting also for the migration in x_L and p_T of the neutron. The solid curve model include the same effects, adding also exchange of ρ and a_2 mesons. Both models give a good description of the large depletion of LN in photoproduction relative to DIS seen in the left side of the figure.

5 Pion structure function

Analogous to the inclusive proton structure function $F_2(Q^2, x)$, one can define an LN tagged semi-inclusive structure function $F_2^{LN}(Q^2, x, x_L)$, including also the dependence on the LN

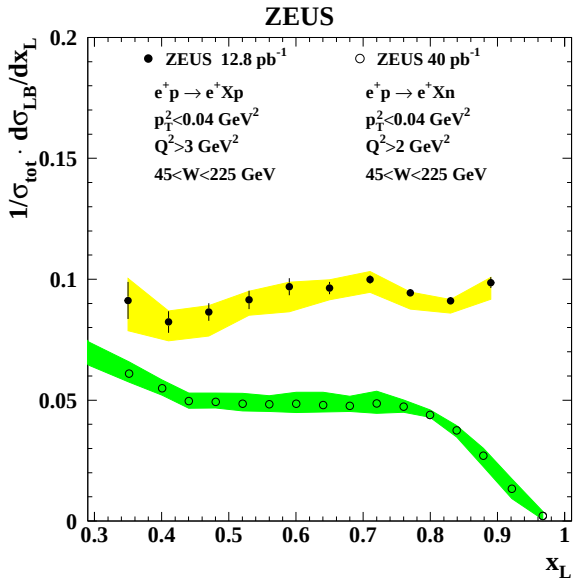

Fig. 3: LP and LN x_L distributions for $p_T^2 < 0.04$ GeV^2.

energy. The left side of Fig. 6 shows the ratios F_2^{LN}/F_2 as a function of Q^2 in bins of x and x_L. Here F_2^{LN} are the measured values from LN production in DIS and the values of F_2 are obtained from the H1-2000 parameterization [5]. For fixed x_L the ratios are almost flat for all (x, Q^2) implying that F_2^{LN} and F_2 have a similar (x, Q^2) behavior. This result suggests the validity of factorization, i.e. independence of the photon and the proton vertices. The statistical precision of the data precludes sensitivity to absorptive effects as discussed in the previous section.

Based on the assumption that at high x_L LN production is dominated by the pion exchange mechanism, the measurement of F_2^{LN} can provide important information about the pion structure. The quark and gluon distributions of the pion have previously been constrained using Drell–Yan and direct photon production data obtained by πp scattering experiments and are limited to high x values $x > 0.1$.

Using the measurement of $F_2^{LN(3)}$ for $0.68 < x_L < 0.77$, and the integral over t of the pion flux factor at the center of this x_L range, $\Gamma_\pi = \int f_{\pi/p}\, dt = 0.131$, one can estimate the pion structure function at low Bjorken–x. Assuming that the Regge model of leading neutron production is valid, the quantity $F_2^{LN(3)}/\Gamma_\pi$ can be associated to the structure function of the pion. The right side of Fig. 6 shows $F_2^{LN(3)}/\Gamma_\pi$ as a function of $\beta = x/(1 - x_L)$ for fixed values of Q^2. The results are consistent with a previous ZEUS measurement [6], where two extreme choices of the pion flux were used to extract F_2^π. The data are compared to predictions of parameterizations of the pion structure function [7]. The measurements are also compared to the H1-2000 parameterization of the proton structure function [5] which is multiplied by the factor 2/3 according to naive expectation based on the number of valence quarks in the pion and proton respectively. The distributions show a steep rise with decreasing β, in accordance with the

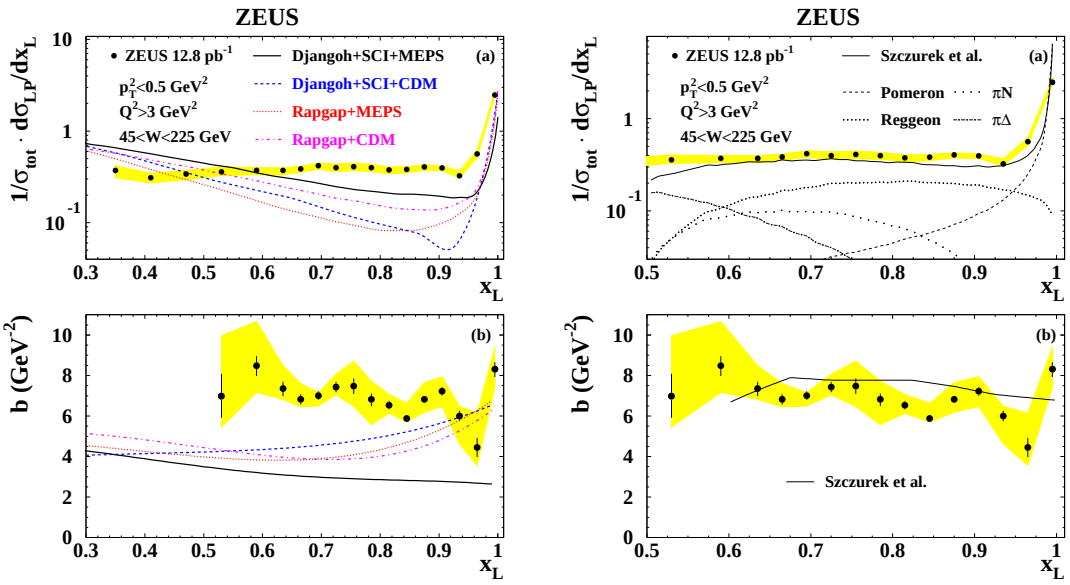

Fig. 4: Left: LP x_L distribution and exponential slopes compared to standard fragmentation models. Right: LP x_L distribution and exponential slopes compared to a model incorporating isoscalar and isovector exchanges.

pion and the proton structure function parameterizations. The scaled proton structure function gives the best description of the data. In absolute values, the presented data are slightly below the expectations, suggesting that additional phenomena, like absorption, may play a role.

References

[1] ZEUS Coll., S. Chekanov et al., Nucl. Phys. **B 776**, 1 (2007);
H1 Coll., contribution to ICHEP-08, H1prelim-08-111;
ZEUS Coll., *Leading proton production in deep inelastic scattering at HERA*, to be published;
and refernces cited therein.

[2] A. Szczurek, N.N. Nikolaev and J. Speth, Phys. Lett. **B 428**, 383 (1998).

[3] N.N. Nikolaev, J. Speth and B.G. Zakharov, Preprint KFA-IKP(TH)-1997-17 (hep-ph/9708290) (1997);
U. D'Alesio and H.J. Pirner, Eur. Phys. J. **A 7**, 109 (2000).

[4] V.A. Khoze, A.D. Martin and M.G. Ryskin, Eur. Phys. J. **C 48**, 797 (2006).

[5] H1 Coll., C. Adloff et al., Eur. Phys. J. **C 21**, 33 (2001).

[6] ZEUS Coll., S. Chekanov et al., Nucl. Phys. **B 637**, 3 (2002).

[7] P. Aurenche et al., Phys. Lett. **B 233**, 517 (1989);
M. Glück, E. Reya and I. Schienbein, Eur. Phys. J. **C 10**, 313 (1999).

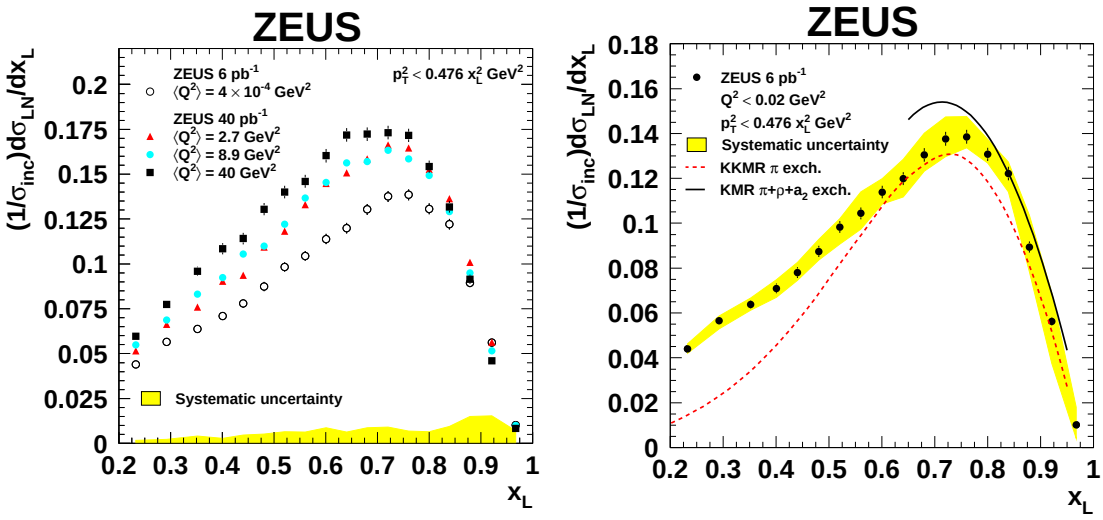

Fig. 5: Left: LN x_L distributions for photoproduction and three bins of Q^2 in DIS. Right: LN x_L distributions for photoproduction compared to exchange models including absorptive effects.

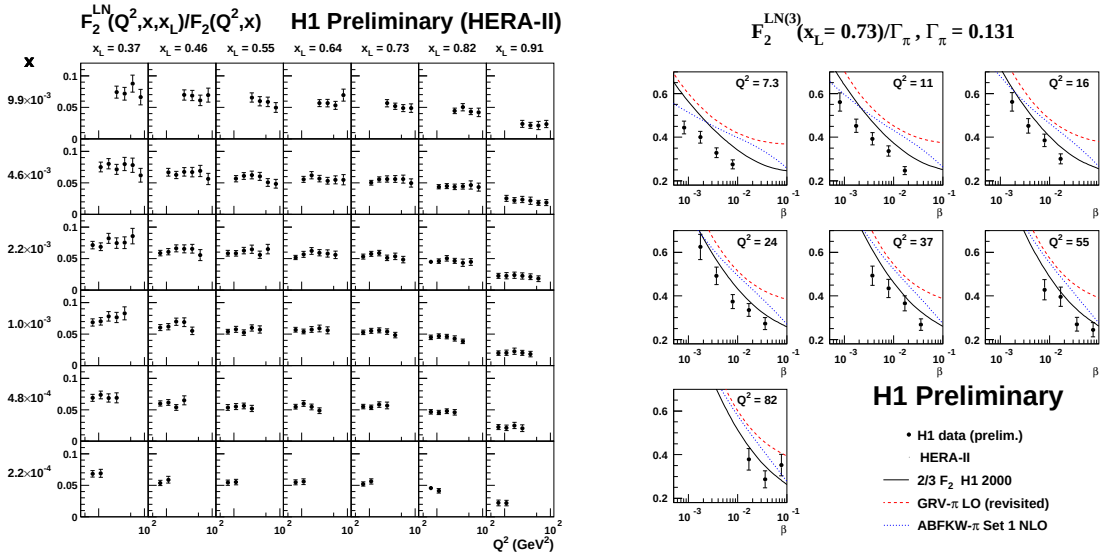

Fig. 6: Left: Ratio of semi-inclusive LN to inclusive structure functions as a function of Q^2 in bins of x and x_L. Right: Extracted pion structure function as a function of $\beta = x/(1 - x_L)$ in bins of Q^2. The curves are the proton structure function scaled by 2/3 and two parameterizations based on Drell-Yan and direct photon production data.